CHARACTERIZATION OF SYNCHRONIZED SPATIOTEMPORAL STATES IN COUPLED NONIDENTICAL COMPLEX GINZBURG–LANDAU EQUATIONS

J. BRAGARD

Department of Physics, University of Liege, Liege, Belgium

F. T. ARECCHI

Istituto Nazionale di Ottica, Largo E. Fermi, 6, I50125 Florence, Italy
Department of Physics, University of Florence, Florence, Italy

S. BOCCALETTI

Department of Physics and Applied Mathematics, Universidad de Navarra,
Irunlarrea s/n, 31080 Pamplona, Spain

We characterize the synchronization of two nonidentical spatially extended fields ruled by one-dimensional Complex Ginzburg–Landau equations, in the two regimes of phase and amplitude turbulence. If two fields display the same dynamical regime, the coupling induces a transition to a completely synchronized state. When, instead, the two fields are in different dynamical regimes, the transition to complete synchronization is mediated by defect synchronization. In the former case, the synchronized manifold is dynamically equivalent to that of the unsynchronized systems, while in the latter case the synchronized state substantially differs from the unsynchronized one, and it is mainly dictated by the synchronization process of the space-time defects.

1. Introduction

Synchronization of concentrated chaotic systems has been the subject of a large body of recent investigations. It has been demonstrated that coupled chaotic concentrated systems may display four levels of synchronization, namely complete synchronization (CS) [Pecora & Carroll, 1990], phase synchronization (PS) [Rosenblum *et al.*, 1996], lag synchronization (LS) [Rosenblum *et al.*, 1997], and generalized synchronization (GS) [Rulkov *et al.*, 1995]. In CS, a perfect hooking of the chaotic trajectories of two systems is achieved by means of a coupling signal, in such a way that they remain in step with each other in the course of time. This mechanism has been shown to occur when two identical chaotic systems are coupled, provided that all the sub-Liapunov exponents of the subsystem to be synchronized are negative [Pecora & Carroll, 1990].

A coupling of nonidentical systems can induce a regime (PS), wherein a locking of the phases is produced, while the amplitudes remain uncorrelated [Rosenblum *et al.*, 1996]. The transition to such a state has been characterized for the Rössler attractor [Rosenblum *et al.*, 1997; Rosa *et al.*, 1998].

LS is an intermediate step between PS and CS. In this case, the two signals lock their phases and amplitudes, but with a time lag [Rosenblum *et al.*, 1997].

The generic scenario for symmetrically coupled nonidentical concentrated systems yields successive

transitions between PS, LS and CS as the coupling parameter is increased [Rosenblum *et al.*, 1997].

Finally, GS implies the hooking of the output of one system to a given function of the output of the other [Rulkov *et al.*, 1995].

The natural continuation of these pioneering works has been to investigate synchronization phenomena in spatially extended systems. Due to the great variety and different classes of extended dynamical systems, a general study would be impracticable, while some information on the main dynamical mechanisms ruling synchronization can be achieved from the study of particular examples. Often, a system close to a bifurcation point is described by means of a normal form equation. As an example, we consider the normal form in the vicinity of an oscillatory instability. In such a condition, a general description of the oscillatory medium is given by the Complex Ginzburg–Landau Equation (CGLE).

Another alternative approach for studying space-time systems consists in connecting a set of concentrated chaotic systems by means of a given coupling (e.g. diffusive coupling) between the individuals constituting the set. Space-time chaos synchronization has been studied for populations of coupled dynamical systems [Pikovsky *et al.*, 1996], for systems formed by globally coupled Hamiltonian or bistable elements [Zanette, 1997], and for neural networks [Zanette & Mikhailov, 1998].

Coming back to continuous systems, the emergence of synchronized states has been investigated for one-dimensional chemical models [Parmananda, 1997], and for two fields obeying identical one-dimensional Complex Ginzburg–Landau Equations [Amengual *et al.*, 1997]. In particular, Amengual *et al.* [1997] report another type of synchronization, called generalized synchronization, consisting of the hooking of the amplitude of one system to a given function of the amplitude of the other system.

A natural question arises: Is it possible to realize all different kinds of synchronization features in the case of a coupling between nonidentical extended systems? This problem has been only recently addressed [Boccaletti *et al.*, 1999; Chaté *et al.*, 1999]. In this paper, we first summarize the results already reported by us in [Boccaletti *et al.*, 1999], and then present further analysis and a detailed discussion for the synchronization states emerging in the particular case of large parameter mismatches.

2. The Model System

For the sake of exemplification, we will refer to a pair of one-dimensional fields $A_{1,2}(x, t)$, each one evolving in space and time via the Complex Ginzburg–Landau Equation (CGL). Such equation describes the dynamical behavior close to the emergence of an "extended" Hopf bifurcation. It has been used to model many different situations in laser physics, fluid dynamics, chemical turbulence, and also to model a chain of coupled oscillators.

The system under study is

$$\dot{A}_{1,2} = A_{1,2} + (1 + i\alpha_{1,2})\partial_x^2 A_{1,2}$$
$$- (1 + i\beta_{1,2})|A_{1,2}|^2 A_{1,2} + \varepsilon(A_{2,1} - A_{1,2}),$$
(1)

where $A_{1,2}(x, t) \equiv \rho_{1,2}(x, t)e^{(i\psi_{1,2}(x,t))}$ are two complex fields of amplitudes $\rho_{1,2}$ and phases $\psi_{1,2}$ respectively, $\partial_x^2 A_{1,2}$ stays for the second derivative of $A_{1,2}$ with respect to the space variable $0 \leq x \leq L$, L represents the system size, dot denotes temporal derivative, $\alpha_{1,2}$, $\beta_{1,2}$ are suitable real parameters, and ε is the strength of the symmetric coupling.

For $\varepsilon = 0$, Eq. (1) describes the evolution of two uncoupled fields $A_{1,2}$, each one obeying a separate CGL. It is a known result that such an equation has plane wave solutions of the form $A_q = \sqrt{1 - q^2}\, e^{i(qx + \omega t)}$ ($-1 \leq q \leq 1$ is the wavenumber in the Fourier space, and $\omega = -\beta - (\alpha - \beta)q^2$). In the parameter region $\alpha\beta > -1$ and outside the range $-q_c \leq q \leq q_c$ ($q_c = \sqrt{(1 + \alpha\beta/2(1 + \beta^2) + 1 + \alpha\beta)}$), these solutions become unstable through the so-called Eckhaus instability. q_c vanishes as soon as the product $\alpha\beta$ approaches -1, thus meaning that all plane waves become unstable when crossing below the $\alpha\beta = -1$ line in the parameter space, which is called *Benjamin–Feir* line. Above this line, three different turbulent states can be identified, namely phase turbulence (PT), amplitude or defect turbulence (AT), and bichaos. We will specialize our analysis on PT and AT, since they have received special attention in the scientific community [Montagne *et al.*, 1997; Torcini, 1997].

The PT regime is obtained just above the $\alpha\beta = -1$ line, and is characterized by a chaotic evolution for the phase ψ, whereas the amplitude ρ remains always bounded away from zero. By going further away from the Benjamin–Feir line, the system experiences a transition toward AT. In this new regime the amplitude dynamics becomes dominant, implying the occurrence of large amplitude

variations which can occasionally drive ρ to zero, thus giving rise to space-time defects.

The effect of $\varepsilon \neq 0$ in Eq. (1) was studied by Boccaletti *et al.* [1999]. We herewith summarize the main results. It is important to remark that we deal here with nonidentical systems ($\alpha_1 \neq \alpha_2$, $\beta_1 \neq \beta_2$), so that two different cases must be taken into account, namely the small and large parameter mismatch cases. For small parameter mismatches, the systems are prepared in the same dynamical regime, e.g. both in PT or in AT. On the contrary, for large parameter mismatches, α_1, α_2, β_1, β_2 are chosen so that one system is in the PT regime, while the other is in the AT regime.

3. Small Parameter Mismatch

3.1. *AT–AT case*

We first consider small parameter mismatches, and select $\alpha_1 = \alpha_2 = 2.1$, $\beta_1 = -1.25$, $\beta_2 = -1.2$ in Eq. (1) (both fields in AT). Figure 1 reports the space-time plots of ρ_1 (a, d, g), ρ_2 (b, e, h)$|\rho_1 -$ $\rho_2|$(c, f, l) for $\varepsilon = 0.05$ (a, b, c), $\varepsilon = 0.09$ (d, e, f) and $\varepsilon = 0.15$ (g, h, l). In all cases, the patterns come out from a codification into a 256 gray-level scale. The dark lines in (a, b, d, e, g, h) trace the positions of the space-time defects. The simulations of Eq. (1) have been performed with $L = 64$, periodic boundary conditions and random initial conditions. The numerical code is based on a semi-implicit scheme in time with finite differences in space. The precision of the code is first-order in time and second-order in space. A space discretization $\delta x = 0.125$ (512 mesh points) and an integration time step $\delta t = 0.001$ have been used. From Fig. 1 one can infer the existence of a gradual passage from a nonsynchronized AT state (a, b, c) to a completely synchronized AT state (g, h, l), through an intermediate state (d, e, f) wherein partial synchronization is built. Notice that here the synchronization of the global structure implies the synchronization of each localized space-time defect.

At variance with what happens in concentrated systems, here the transition from nonsynchronized to synchronized states is not associated with the
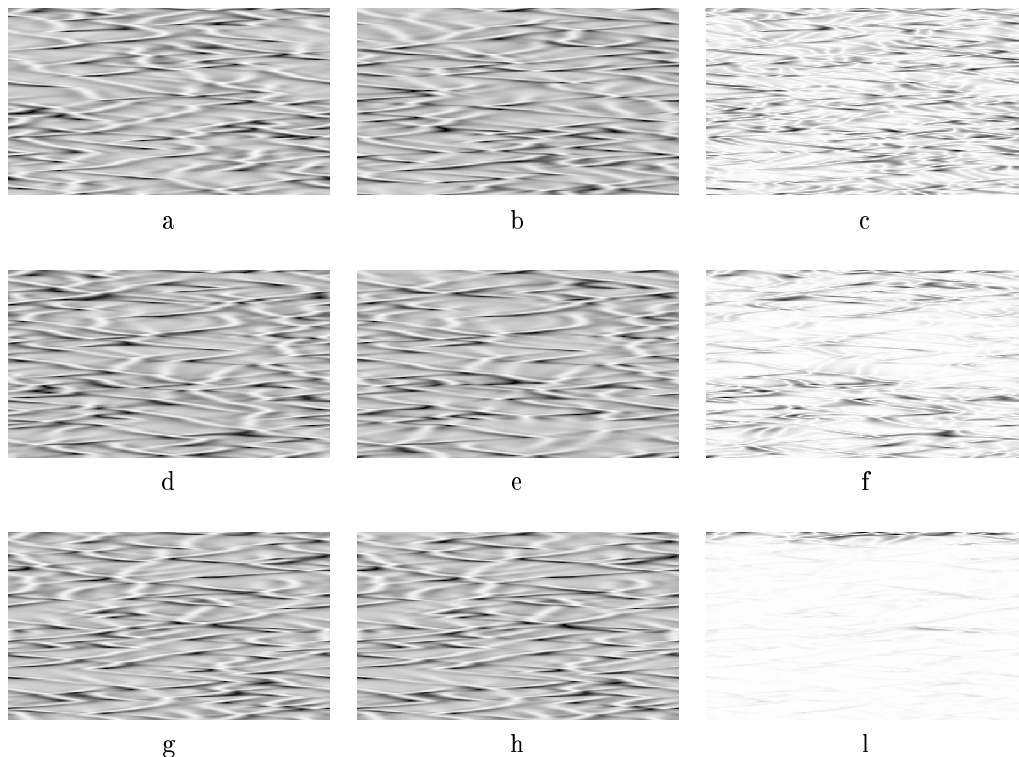

Fig. 1. AT–AT Case: Space (horizontal)-time(vertical) plots of (a, d, g) ρ_1, (b, e, h) ρ_2 and (c, f, l) $-|\rho_1 - \rho_2|$. $\alpha_1 = \alpha_2 = 2.1$, $\beta_1 = -1.25$, $\beta_2 = -1.2$. Time increases downwards from 300 to 600 (u.t.). The first 300 time units (not plotted) corresponds to the transient before the system reaches two independent chaotic (AT) states starting from two independent random initial conditions. (a, b, c) correspond to $\varepsilon = 0.05$, (d, e, f) to $\varepsilon = 0.09$, (g, h, l) to $\varepsilon = 0.15$. In (c, f, l) the white regions correspond to $|\rho_1 - \rho_2| = 0$, that indicates complete synchronization.
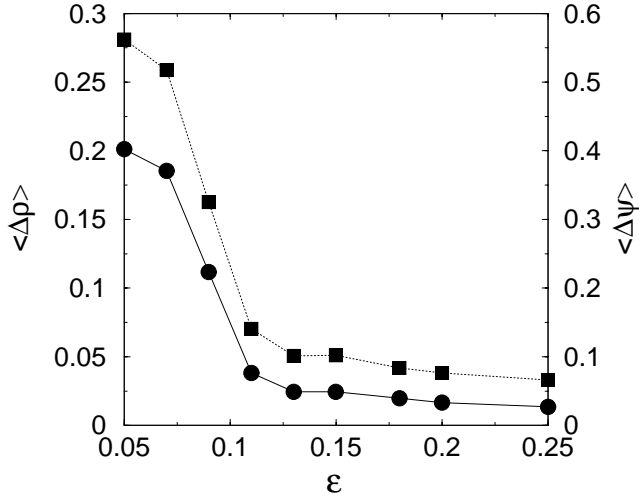
Fig. 2.   AT–AT Case: Indicators of modulus (circles) and phase (squares) synchronization. Space-time average of the difference between amplitudes and phases of the two fields versus the coupling ε (see definitions in the text). Same parameters as in the caption of Fig. 1. The left (right) vertical axis reports the $\langle \Delta \rho \rangle$ ($\langle \Delta \psi \rangle$) scale.

presence of an intermediate PS regime. To quantitatively show this feature, we report in Fig. 2 the measurements of $\langle \Delta \rho \rangle = \langle |\rho_1 - \rho_2| \rangle$ and $\langle \Delta \psi \rangle = \langle |\psi_1 - \psi_2| \rangle$ as functions of ε ($\langle \cdots \rangle$ stays for an averaging in both time and space). From Fig. 2 one infers that $\langle \Delta \rho \rangle(\varepsilon)$ and $\langle \Delta \psi \rangle(\varepsilon)$ gradually decay at once. The scenario is therefore consistent with what is already observed for small parameter mismatches in chemical models [Parmananda, 1997].

3.2. *PT–PT case*

The scenario does not qualitatively change when we consider the coupling between two initial PT states. Let us choose $\alpha_1 = \alpha_2 = 2.1$, $\beta_1 = -0.75$, $\beta_2 = -0.83$ in Eq. (1) (both fields in PT), and, by gradually increasing ε, perform simulations with the same system size, boundary conditions and initial conditions as above. The results are shown in Fig. 3, where we report ρ_1 (a and d) , ρ_2 (b and e) $|\rho_1 - \rho_2|$ (c and f) for two values of the coupling parameter $\varepsilon = 0.02$ (a, c, b) and $\varepsilon = 0.04$ (d, e, f). Here again, the system passes from a unsynchronized PT state at small couplings to a completely synchronized PT state. In this case, since defects are not present, the synchronization is global and it emerges for a smaller coupling strength.

4.   Large Parameter Mismatch

A much more interesting scenario has been observed in the case of large parameter mismatches. Let us select in Eq. (1) $\alpha_1 = \alpha_2 = 2.1$, $\beta_1 = -1.2$, $\beta_2 = -0.83$. This implies that the field A_1 is evolving in AT, while the field A_2 is evolving in PT. In Fig. 4 we report the patterns arising from the space-time representations of ρ_1 (a, d, g), ρ_2 (b, e, h) $|\rho_1 - \rho_2|$ (c, f, l) for $\varepsilon = 0.03$ (a, b, c), $\varepsilon = 0.14$ (d, e, f) and $\varepsilon = 0.19$ (g, h, l).

At small coupling strengths, the two systems do not synchronize, and they hold in their respective regimes [Figs. 4(a)–4(c)]. At large coupling
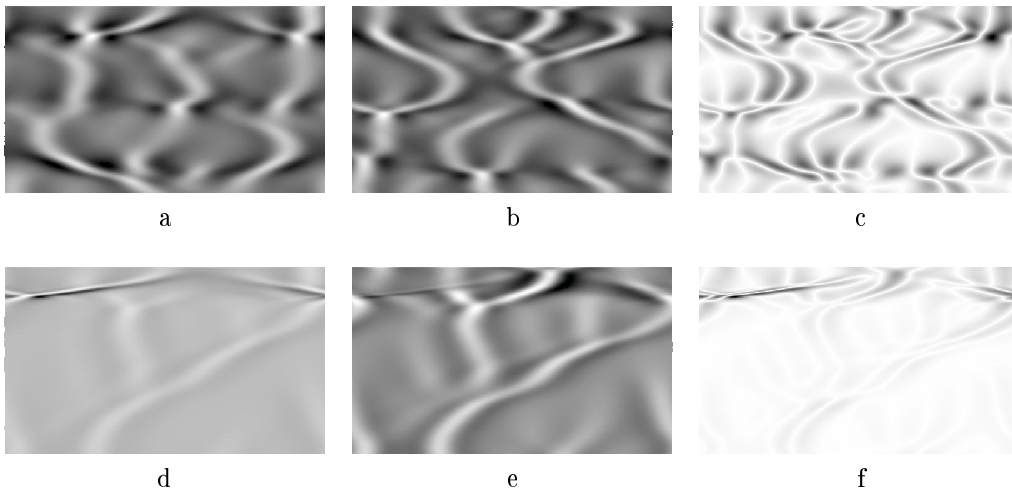

Fig. 3.   PT–PT Case: Space (horizontal)-time(vertical) plots of (a, d) ρ_1, (b, e) ρ_2, and (c, f) $-|\rho_1 - \rho_2|$. $\alpha_1 = \alpha_2 = 2.1$, $\beta_1 = -0.75$, $\beta_2 = -0.83$. Other parameters, initial conditions and boundary conditions as in Fig. 1. Same stipulations as in Fig. 1. (a, b, c) correspond to $\varepsilon = 0.02$, (d, e, f) to $\varepsilon = 0.04$.
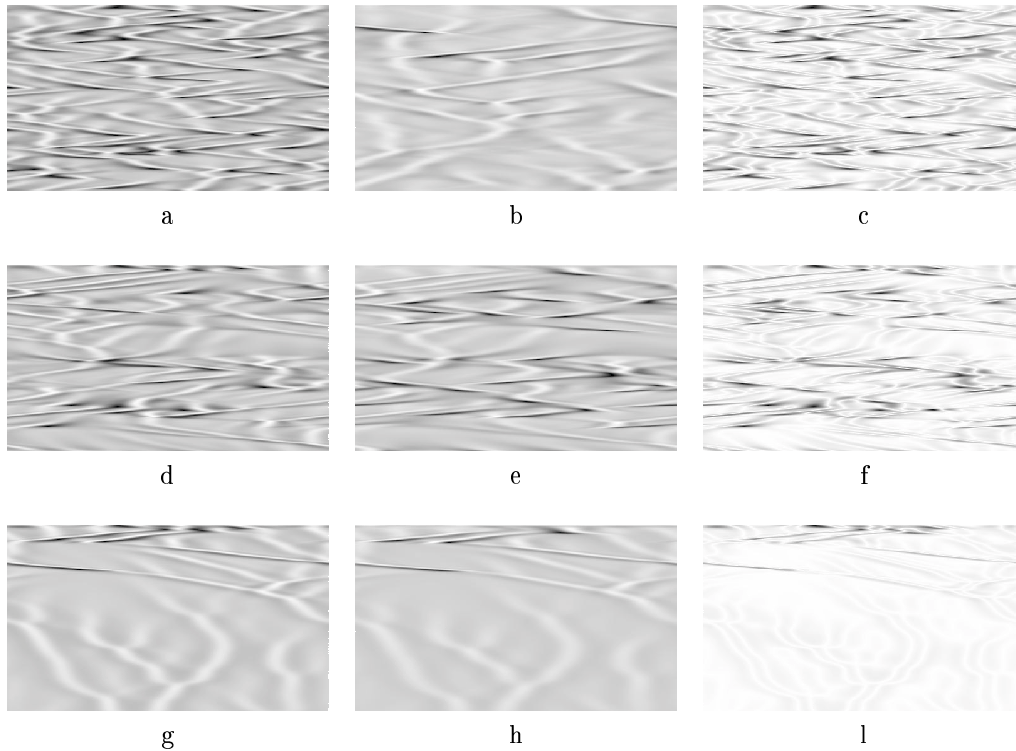
Fig. 4. AT–PT Case: Space (horizontal)-time(vertical) plots of (a, d, g) ρ_1, (b, e, h) ρ_2, and (c, f, l) $-|\rho_1-\rho_2|$. $\alpha_1 = \alpha_2 = 2.1$, $\beta_1 = -1.2$, $\beta_2 = -0.83$. Other parameters, initial conditions and boundary conditions as in Figs. 1 and 3. Same stipulations as in Figs. 1 and 3. (a, b, c) correspond to $\varepsilon = 0.03$, (d, e, f) to $\varepsilon = 0.14$, (g, h, l) to $\varepsilon = 0.19$.

strengths, the two systems reach a CS regime, which is realized in PT [Figs. 4(g)–4(l)]. This implies that the final synchronized state is space-time chaotic, but the synchronization process is here associated with the suppression of all defects, which were initially present in the field A_1.

In other words, since CS implies both amplitude and phase synchronization, the small amplitude oscillations of A_2 attract the synchronized set, and, as a result, the defects originally existing in the dynamics of A_1 are suppressed.

However, the most interesting regime comes out to be the intermediate one [Figs. 4(d)–4(f)], wherein the two systems organize so as to produce a partial synchronization, which is realized in an AT regime. The above-said is further confirmed by the plots of $\langle\Delta\rho\rangle$ and $\langle\Delta\psi\rangle$ as functions of ε (see Fig. 5). At variance with Fig. 2, a quite wide range of ε can be isolated ($0.1 \leq \varepsilon \leq 0.16$), wherein amplitude synchronization is not yet reached [see Fig. 4(f)], while the average phase distance converges to a constant value. In this situation, one expects that the amplitudes of the two fields can be uncorrelated, while the phases are already strongly coupled.
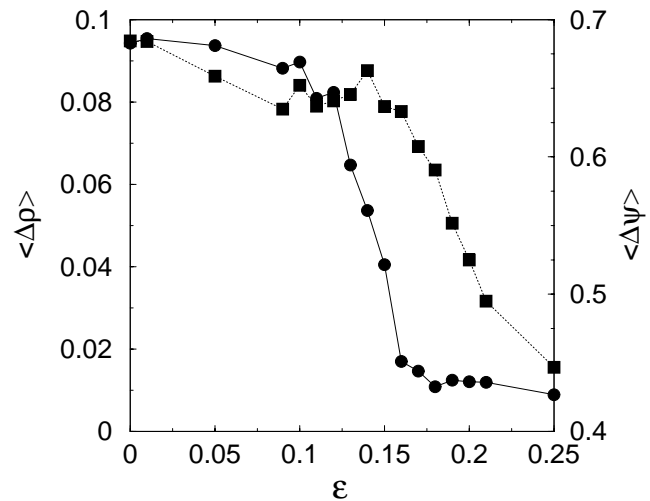

Fig. 5. AT–PT Case: Indicators of modulus (circles) and phase (squares) synchronization (same stipulations as in Fig. 2). Parameters, initial and boundary conditions as in the caption of Fig. 4. Note the phase plateau for $0.1 \leq \varepsilon \leq 0.16$.

An heuristic argument for such a phenomenon can be offered. The natural evolution of A_1 is in AT, that is showing the presence of many space-time defects. As already discussed, defects are localized

points wherein the amplitude of the field vanishes. As a consequence, in each one of them, the phase ψ_1 shows a singularity.

One can now imagine that AT allows flexibility in the dynamics of the amplitude, but the variations of the phase are not flexible, since they are substantially determined by the local amplitude variations. On the contrary, A_2 would naturally evolve in PT, that is with a dominant phase dynamics. The phase ψ_2 is not naturally bounded, and its oscillations are allowed by the evolution of the uncoupled systems. For $0.1 \leq \varepsilon \leq 0.16$, a strong correlation is built in the phases. There, ψ_1 and ψ_2 converge in average (apart from a constant). This is possible only when ψ_2 locally adjusts on ψ_1. The relevant consequence of this process is the introduction of many defects in the field A_2, which would be instead free of them in the uncoupled state.

The conclusion is that, while for small parameter mismatches one observes a passage from unsynchronized to completely synchronized states, for large parameter mismatches, this transition is mediated by a state which is similar to what was called phase synchronization for concentrated systems. In the former case, the resulting space-time synchronized state is not qualitatively different from the unsynchronized one, in the latter case, the state of the system resulting from the synchronization process may substantially differ from that present with no coupling, and it is mainly dictated by the synchronization process of the space-time defects. The above body of results have been presented in [Boccaletti *et al.*, 1999]. In the following we will analyze more deeply the features of this latter case, and try to isolate the main spatial and temporal components of it.

5. Quantitative Indicators for Synchronization

The first step of our analysis is to quantitatively confirm the above qualitative picture for the large parameter mismatch case. For this purpose we measure the total number of phase defects N_d as a function of ε for $\alpha_1 = \alpha_2 = 2.1$, $\beta_1 = -1.2$, $\beta_2 = -0.83$. Figure 6 reports N_d versus ε for A_1 (circles) and A_2 (squares). At small coupling strengths $(0 < \varepsilon < 0.1)$ the two fields evolve in an unsynchronized manner. At intermediate ε values $(0.1 < \varepsilon < 0.16)$ a process of defect injection into the field A_2 up to the point $(\varepsilon \simeq 0.16)$ is
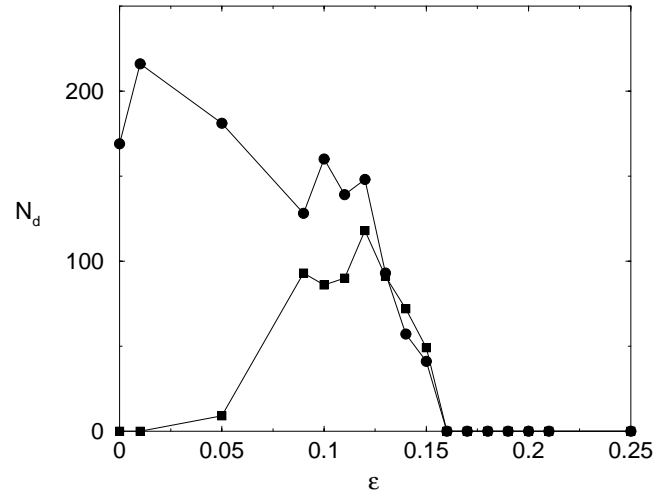

Fig. 6.   AT–PT Case: Total number of phase defects N_d as a function of the coupling strength ε for A_1 (circles) and A_2 (squares). Same parameters, initial and boundary conditions as in the caption of Fig. 4.

evident where both fields show the same defect number. Notice that this ε range coincides exactly with the phase plateau in Fig. 5. Finally, when all defects have been synchronized, the system begins to reach a CS state, which is realized in PT, implying the absence of phase defects in both fields (as it is evident from Fig. 6).

Up to now we have considered only global indicators, that is averages on both space and time, so a natural question emerges: Is this synchronization phenomenon a temporal phenomenon, a spatial phenomenon or a spatiotemporal phenomenon? To answer this question we have to analyze separately the space and time effects entering the process of pattern synchronization. Therefore, we go in the Fourier space $(x \to k,\ t \to \Omega)$ and we consider $\tilde{A}_{1,2}(k,\ \Omega)$, that is the Fourier transforms of the fields $A_{1,2}(x,\ t)$. In this new space, we can separately investigate time and space effects. For each ε value, let us consider the following mean quantities

$$\langle k \rangle_{1,2}(\varepsilon) \equiv \frac{1}{N_{1,2}} \int_{-k_m}^{+k_m} \int_{-\Omega_m}^{+\Omega_m} k |\tilde{A}_{1,2}(k,\ \Omega)|^2 \mathrm{d}k \mathrm{d}\Omega\,,$$

$$\langle \Omega \rangle_{1,2}(\varepsilon) \equiv \frac{1}{N_{1,2}} \int_{-k_m}^{+k_m} \int_{-\Omega_m}^{+\Omega_m} \Omega |\tilde{A}_{1,2}(k,\ \Omega)|^2 \mathrm{d}k \mathrm{d}\Omega\,,$$

$$(2)$$

where $\Omega_m \equiv (N\pi/t_t)$, $k_m \equiv (N\pi/L)$, N is the total number of discrete data considered for the Fourier transform, t_t is the total running time of the simulation, and the normalization constants $N_{1,2}$ are
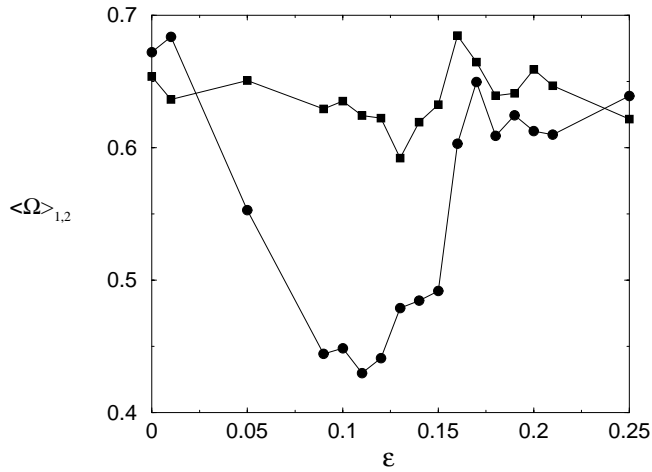
Fig. 7. AT–PT Case: $\langle\Omega\rangle_1$ (squares) and $\langle\Omega\rangle_2$ (circles) as functions of ε (see text for definitions). $\alpha_1 = \alpha_2 = 2.1$, $\beta_1 = -1.2$, $\beta_2 = -0.83$. Other parameters, initial and boundary conditions as in the caption of Fig. 4.

defined by

$$N_{1,2} \equiv \int_{-k_m}^{+k_m} \int_{-\Omega_m}^{+\Omega_m} |\tilde{A}_{1,2}(k, \Omega)|^2 \mathrm{d}k\mathrm{d}\Omega. \qquad (3)$$

Notice that both Ω_m and k_m depend on the particular discretization used in the simulations. The results for the large parameter mismatch case show that $\langle k\rangle_{1,2}(\varepsilon) \simeq 0$ independently on ε, as one should have expected considering the fact that turbulent regimes in the CGL come out from large wavelength instabilities. On the contrary, the quantities $\langle\Omega\rangle_{1,2}$ are always bounded away from zero and strongly depend on the coupling strength. Figure 7 reports $\langle\Omega\rangle_1$ (squares) and $\langle\Omega\rangle_2$ (circles) as a function of ε for $\alpha_1 = \alpha_2 = 2.1$, $\beta_1 = -1.2$, $\beta_2 = -0.83$. While the field A_1 appears to be robust in the variation of its temporal frequency, the field A_2 shows a large
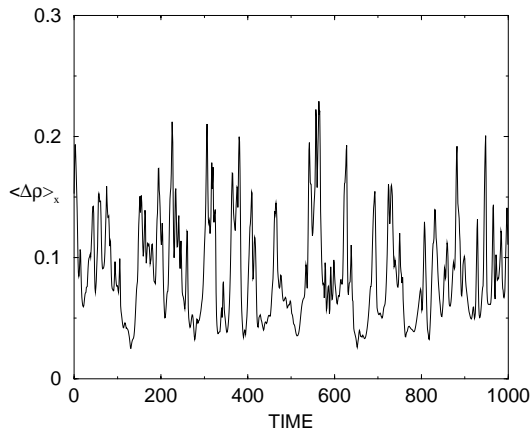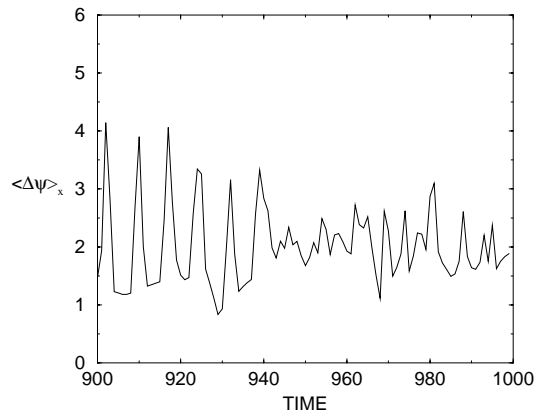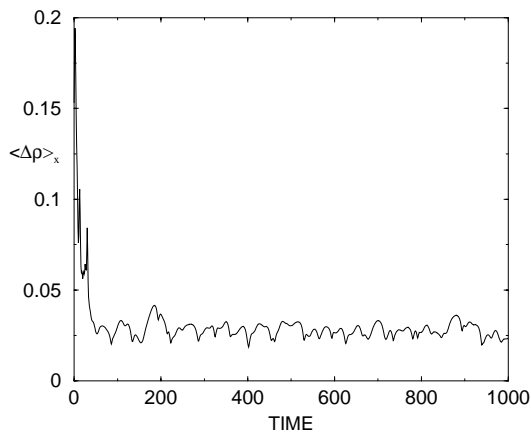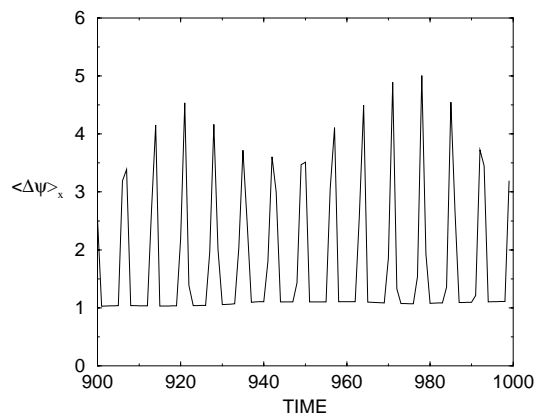

Fig. 8. AT–PT Case: (a, c) $\langle|\rho_1 - \rho_2|\rangle_x$ and (b, d) $\langle|\psi_1 - \psi_2|\rangle_x$ versus time (see text for definitions) for (a, b) $\varepsilon = 0.14$ and (c, d) $\varepsilon = 0.17$. $\alpha_1 = \alpha_2 = 2.1$, $\beta_1 = -1.2$, $\beta_2 = -0.83$. Other parameters, initial and boundary conditions as in the caption of Fig. 4.

variation in its frequency as a function of the coupling, thus confirming our heuristic argument about the flexibility of A_2 during the synchronization process. Figure 7 also indicates that the whole synchronization scenario should be regarded as mainly dictated by temporal effects.

This suggests to consider only spatial averages for $|\rho_1 - \rho_2|$ and $|\psi_1 - \psi_2|$, as opposed to what we have considered in Figs. 2 and 5, and to investigate the temporal evolution of such new average differences at different ε values.

Let us then define $\langle|\rho_1 - \rho_2|\rangle_x(t)$, $\langle|\psi_1 - \psi_2|\rangle_x(t)$ the spatial averages of the differences in amplitudes and phases of the two fields (now $\langle\cdots\rangle_x$ indicates an averaging only along the spatial variable x). In Fig. 8 we show how $\langle|\rho_1 - \rho_2|\rangle_x(t)$ (a and c) and $\langle|\psi_1 - \psi_2|\rangle_x(t)$ (b and d) evolve in time for $\varepsilon = 0.14$ (a and b) and $\varepsilon = 0.17$ (c and d), that is immediately before and after the point $\varepsilon \simeq 0.16$ for which both fields show the same defect number N_d (see Fig. 6). From Fig. 8 one can clearly appreciate that the transition toward a completely synchronized state (occurring for $\varepsilon > 0.16$) corresponds to the appearance of a regular periodic behavior for the spatial average of the difference in phase. Correspondingly, the fluctuations of $\langle|\rho_1 - \rho_2|\rangle_x(t)$ are strongly washed out, again as one should have expected by considering that the system passes from an amplitude ($\varepsilon < 0.16$) to a phase ($\varepsilon > 0.16$) turbulent state, and that, in this latter state the dominant dynamics is the phase dynamics. It is important to remark that, while Fig. 8 depicts the behavior of the system close to the transition, from Fig. 5 one can appreciate that the spatiotemporal average $\langle\Delta\psi\rangle$ further decreases for increasing $\varepsilon > 0.17$. Therefore, a question arises on how the temporal behavior of $\langle|\psi_1 - \psi_2|\rangle_x(t)$ accompanies the decreasing process of $\langle\Delta\psi\rangle$, and on whether the amplitude fluctuations of $\langle|\psi_1 - \psi_2|\rangle_x(t)$ decrease, eventually vanishing at very large ε values. The results of this investigation will be reported elsewhere.

6. Conclusions

We have discussed the emergence of synchronization features in a pair of coupled nonidentical spatially extended pattern forming systems, with reference to the one-dimensional Ginzburg–Landau Equation, that is referring to a general case of an extended system undergoing an Hopf bifurcation. We have distinguished two main cases, namely the small and large parameter mismatches.

In the small parameter mismatch case, the two uncoupled systems give rise to the same qualitative space-time behavior (they are both either in phase or in amplitude turbulence). In this situation, the coupling induces a gradual transition toward a completely synchronized state, which is realized in the same dynamical regime recovered by the uncoupled systems.

In the large parameter mismatch case, the two systems are prepared with no coupling so that one of them realizes a phase turbulent state, while the other lies within amplitude turbulence. In such a case, high coupling strengths induce a complete synchronized state, which is realized in phase turbulence, that is implying the suppression of all phase defects originally present in the amplitude turbulent field. For intermediate coupling strengths, the systems realize partial synchronization features, and they both give rise to an amplitude turbulent regime. A quantitative analysis of this last case shows that such a regime corresponds to a phase locking, while amplitudes come out to be uncorrelated. A relevant consequence is the injection of many phase defects in the field which was originally free of them. The introduction of suitable indicators for separately analyzing space and time effects allows to highlight that the transition between the two above synchronization states is associated with the emergence of a periodic temporal behavior for the space average of the difference of the two phases.

Acknowledgments

References

Amengual, A., Hernández-García, E., Montagne, R. & San Miguel, M. [1997] "Synchronization of spatiotemporal chaos: The regime of coupled spatiotemporal intermittency," *Phys. Rev. Lett.* **78**, 4379–4382.

Boccaletti, S., Bragard, J., Arecchi, F. T. & Mancini, H. L. [1999] "Synchronization in nonidentical extended systems," *Phys. Rev. Lett.* **83**, 536–539.

Chaté, H., Pikovsky, A. & Rudzick, O. [1999] "Forcing oscillatory media: Phase kinks versus synchronization," *Physica* **D131**, 17–30.

Montagne, R., Hernández-García, E. & San Miguel, M. [1997] "Winding number instability in the phase-turbulence regime of the complex Ginzburg–Landau equation," *Phys. Rev. Lett.* **77**, 267–270.

Parmananda, P. [1997] "Generalized synchronization of spatiotemporal chemical chaos," *Phys. Rev.* **E56**, 1595–1598.

Pecora, L. M. & Carroll, T. L. [1990] "Synchronization in chaotic systems," *Phys. Rev. Lett.* **64**, 821–824.

Pikovsky, A., Rosenblum, M. G. & Kurths, J. [1996] "Synchronization in a population of globally coupled chaotic oscillators," *Europhys. Lett.* **34**, 165–170.

Rosa, E. Jr., Ott, E. & Hess, M. H. [1998] "Transition to phase synchronization of chaos," *Phys. Rev. Lett.* **80**, 1642–1645.

Rosenblum, M. G., Pikovsky, A. & Kurths, J. [1996] "Phase synchronization of chaotic oscillators," *Phys. Rev. Lett.* **76**, 1804–1807.

Rosenblum, M. G., Pikovsky, A. & Kurths, J. [1997] "From phase to lag synchronization in coupled chaotic oscillators," *Phys. Rev. Lett.* **78**, 4193–4196.

Rulkov, N. F., Sushchik, M. M., Tsimring, L. S. & Abarbanel, H. D. I. [1995] "Generalized synchronization of chaos in directionally coupled chaotic systems," *Phys. Rev.* **E51**, 980–994.

Torcini, A. [1997] "Order parameter for the transition from phase to amplitude turbulence," *Phys. Rev. Lett.* **77**, 1047–1050.

Zanette, D. H. [1997] "Dynamics of globally coupled bistable elements," *Phys. Rev.* **E55**, 5315–5320.

Zanette, D. H. & Mikhailov, A. S. [1998] "Mutual synchronization in ensembles of globally coupled neural networks," *Phys. Rev.* **E58**, 872–875.